Modeling Braided Shields via Multipole Representations for the Braid Charges and Currents

W. A. Johnson, W. L. Langston, L. I. Basilio, L. K. Warne*

Abstract — **A first principles calculation for the transfer capacitance of a Beldon cable is carried out by the use of filamentary constant, dipole, quadrupole, and octopole unknown charges placed at the center of each braid wire. Results are compared with full electrostatic simulations and a phenomenological model.**

1 INTRODUCTION

A review of the literature on development of phenomenological models for penetration of cable shields has been documented in [1]. These models have had considerable success in predicting the penetration through cable shields; however, we occasionally run into modifications of cable topology that call into question the use of these models. It would thus be useful to assemble a first principles model of the shield, not only to handle changes in topology from the standard geometry, but also to form a theoretical underpinning for the existing models. The commercially available Beldon cable of Figure 1 was chosen as a generic test problem. As a simpification, the braid is replaced by an infinitely periodic quasi-planar braid. The relationship between the transfer capacitance (C_T) of the coaxial cable and planar shield is given by

$$C_T = -\frac{\phi^{tot}/E_0}{b}\frac{2\pi\varepsilon_0}{\ln(b_{gnd}/b)\ln\left[(b+\phi_c/E_0)/a\right]},$$

where ϕ^{tot} is the potential difference between a point far above the braid and the braid in the planar problem, a is the inner conductor radius, b is the outer shield radius, and b_{gnd} is the effective radius to a ground outside of the braid. A similar relationship holds between the transfer inductance and the magnetic flux of the magnetostatic planar braid problem.

The present work is an extension of [1] where a planar approximation to the cylindrical braid was modeled with Sandia's electrostatic version of EIGER^{TM}. A unit cell for the two-dimensional infinitely periodic problem is shown in Figure 2 . The

Figure 1: A commercially available Beldon cable.

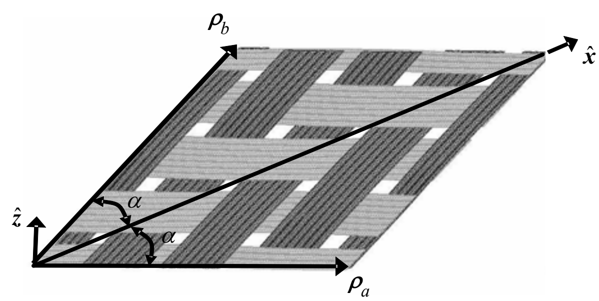

Figure 2: The unit cell of the two-dimensional infinitely periodic braid.

diameter of a single strand is 0.005", the magnitude of both lattice vectors $\boldsymbol{\rho}_a$ and $\boldsymbol{\rho}_b$ is 0.2440474", $\alpha = 24.4°$, and $\widehat{x}$ is along the cable axis. The unit cell area A is $0.044\,813\,2$ in^2. In [1], each of the 56 wires of the unit cell was meshed for simulation with 30 segments along the length and 16 segments around the circumference, giving a total unknown count of 53,760. Due to the large number of unknowns and the need to ultimately set up the the magnetostatic diffusion problem (to be considered in future work), the use of a modal series for the ϕ varation of the currents on each wire was proposed in [1].

The present work is similar in spirit to the modal

*Electromagnetics Effects Department, Sandia National Laboratories, P.O. Box 5800, Mail Stop 1152, Albuquerque, NM, USA 87185-1152 e-mail:wajohns@sandia.gov, tel.: 1-505-844-6329, fax: 1-505-284-6078. Sandia is a multiprogram laboratory operated by Sandia Corporation, a Lockheed Martin Company, for the United States Department of Energy under contract DE-AC04-94AL85000.

series solution but is simpler in its implementation. Piecewise constant filament charge densities, as well as their dipole, quadrupole, and octopole counterparts (extending over each wire segment) are placed along the center of each ($\rho = 0$) segment.

2 FORMULATION OF THE ELECTROSTATIC INTEGRAL EQUATION

We formulate the integral equation for the unknown sources in a single unit cell. Ths sources have the form

$$\sigma^{(i,j)}(\mathbf{s}') = \sum_{n=1}^{Nseg} \sigma_n^{(i,j)} u_n(\mathbf{s}'), \tag{1}$$

where

$$u_n(s) = \begin{cases} 1, \text{ if } s' \text{ in the } n^{th} \text{ segment} \\ 0, \text{ otherwise} \end{cases}. \tag{2}$$

We work in the coordinate system of the n^{th} segment which runs from r_{n-1} to r_n in the global coordinate system and points in the local $\widehat{z}_n$ direction. The other unit vectors in the local wire segment coordinate system are denoted by $\widehat{x}_n$ and $\widehat{y}_n$. They are chosen to make a right handed $\widehat{x}_n, \widehat{y}_n, \widehat{z}_n$ triplet. The index pair (i,j) denotes the multipole index. Thus, a charge filament has indices $(i,j) = (0,0)$. A dipole charge unknown with indices $(1,0)$ indicates a charge displacement in the $\widehat{x}_n$ direction where $(0,1)$ denotes a charge displacement in the $\widehat{y}_n$ direction. For quadrupole charge distributions, the indices $(2,0)$ denote a quadrupole charge in the $\widehat{x}_n$ direction while $(1,1)$ denotes a quadrupole formed by dipole displacement in both the $\widehat{x}_n$ and $\widehat{y}_n$ directions. Due to the near linear dependency of the $(2,0)$ and $(0,2)$ quadrupole source terms, we do not use the $(0,2)$ quadrupole source term. For octopoles we use the $(3,0)$ and $(2,1)$ source terms. This gives $N^{u,seg} = 3$, 5, or 7 independent unknowns for each wire segment for dipoles, quadrupoles, and octopoles, respectively. The potential due to each source term is given by

$$\phi^{tot}(\mathbf{r}) = \phi^{inc}(\mathbf{r}) + \phi^{sc}(\mathbf{r}), \tag{3}$$

where the scattered potential is

$$\phi^{sc}(\mathbf{r}) = \frac{1}{4\pi\varepsilon} \sum_{n=1,}^{N_{seg}} \sum_{i,j} \sigma_n^{(i,j)}. \tag{4}$$

$$\int \left(-\frac{\partial}{\partial y_n}\right)^j \left(-\frac{\partial}{\partial x_n}\right)^i G(\mathbf{r} - \mathbf{r}'(s')) u_n(\mathbf{s}') ds'.$$

Because the tangential component of the electric field vanishes on the surfaces of the individual wires, the total potential must be a constant. This fact is used to solve for the line multipole moments of the wires. The match points on the surface of the m^{th} wire segment are described by

$$\mathbf{r}_{(m,j)} = \mathbf{r}_m^c + a(\cos\varphi_j + \sin\varphi_j \widehat{y}_n), \tag{5}$$

where $\mathbf{r}_m^c$ is the centroid of the m^{th} segment, $-\pi < \varphi_j \leq \pi$ is a local coordinate angle at the wire and a is the wire radius. Since we have $N^{u,seg}$ unknowns on each wire segment, we require $N^{u,seg}$ match points per segment to generate the required equations. We place the match points on the surface of the wire at

$$\varphi_{nj} = 2\pi j / N^{u,seg}, \tag{6}$$

where φ_{nj} is the polar angle in the coordinate system of the n^{th} wire segment and $j = -\frac{N^{u,seg}-1}{2}, -\frac{N^{u,seg}-3}{2}, \ldots, \frac{N^{u,seg}-1}{2}$.

In [1] it was shown that the problem of an $E_z^{inc} = 1$ V incident field below the braid and zero incident field aove the braid may solved by the superposition of two problems. The first problem has a $\widehat{z}$ directed uniform incident field of 0.5 V/m with zero total potential on the braid surface, the total charge q^{UF} on that problem is computed (the superscript 'UF' refers to the uniform field solution for the braid problem). The second problem is that of zero incident field and a unit potential on the braid q^{1V} is computed. The total problem is then solved by setting the braid voltage to be $\phi_{braid} = -(A\varepsilon_0(1V/m) + q^{UF})/q^{1V}$ and incident uniform field excitation $E_z^{inc} = 0.5$ V/m to yield a net field $E_z = 1$ V/m far below the braid and $E_z = 0$ far above the braid.

2.1 Uniform Field and Zero Braid Potential Problem

We now focus attention on the problem of the planar braid excited by a uniform field (3) where the scattered potential $\phi^{sc}(\mathbf{r})$ is given in (4) and the incident potential is

$$\phi^{inc}(\mathbf{r}) = -z/2. \tag{7}$$

We set the $\phi^{tot}(\mathbf{r})$ to zero on the braid surface in (3) to obtain

$$\phi^{sc}\left(r_{(m,j)}\right) = \frac{\widehat{z} \cdot \mathbf{r}_{(m,j)}}{2};\ m = 1, ..., N_{seg}, \tag{8}$$

which is a square linear system for the $N_{seg} \times N^{u,seg}$ unknowns. Once this system is solved for all the charge sources, (3) is used to obtain the scattered potential $\phi^{UF}(\mathbf{r}_0)$ at the observation point $\mathbf{r}_0$ above the braid. The charge σ^{UF} is obtained by summing the product of the charges $\sigma_n^{(0,0)}$ and each segment length Δ_n.

2.2 Zero Uniform Field and Unit Potential Braid Problem

Now a 1 V potential is applied to the braid with zero incident field to yield

$$\phi\left(x_{nj}, y_{nj}, z_n\right) = 1\,,\; n = 1, ..., N_{seg}, \qquad (9)$$

which is again a square linear system for the $Nseg \times N^{u,seg}$ unknowns. Again (3) is used to obtain $\phi^{1V}(r_0)$. The total charge for this excitation q^{1V} is again obtained by summing $\sigma_n^{(0,0)}\Delta_n$ for this excitation. (Here the superscript '1V' refers to the unit potential braid solution.)

2.3 Planar Transfer Capacitance

The total problem has

$$\phi^{braid} = -(\varepsilon_0\ A\ * 1V + q^{UF})/q^{1V}, \qquad (10)$$

and

$$\phi^{tot}(r) = (\phi^{sc,UF}(r) - \frac{\mathbf{r}_z}{2} + (\phi^{1V} - 1.0)\ \phi^{braid}). \qquad (11)$$

The final $\phi^{tot}(r)$ is scaled by 0.0254 $m/inch$ since the units of the braid geometry are provided in inches.

3 EVALUATION OF THE GREEN'S FUNCTIONS BY EWALD METHODS

If $|z - z\prime| < < \max\ (\rho_a, \rho_b)$ as occurs for evaluation of the system matrix elements, the evaluation of the two-dimensional infinitely periodic Green's function is carried out by a static modification to the Ewald methods discussed in [2]. These techniques are used to obtain the doubly-infinite, periodic Green's function for the three-dimensional "planar" braid $G(\mathbf{r}, \mathbf{r}')$ and its gradients $\nabla G(\mathbf{r}, \mathbf{r}')$, $\nabla\nabla G(\mathbf{r}, \mathbf{r}')$, and $\nabla\nabla\nabla G(\mathbf{r}, \mathbf{r}')$ that are needed for the dipole, quadrupole, and octopole sources, respectively. In what follows m_0, n_0 are chosen so that

$$R_{m,n} = |\mathbf{r} - \mathbf{r}' - (m\boldsymbol{\rho}_a + n\boldsymbol{\rho}_b)|$$

is minimized and for simplicity we write $\mathbf{r}$ for $\mathbf{r} - \mathbf{r}'$ and the same for each of its components. Due to space limitations, only a brief summary of the results for $G(\mathbf{r}, \mathbf{r}')$ and $\nabla G(\mathbf{r}, \mathbf{r}')$ are given. Also we need

$$\mathbf{k}_{tmn} = \frac{2\pi}{A} m\boldsymbol{\rho}_b \times \widehat{z} + n\widehat{z} \times \boldsymbol{\rho}_a,$$

for the spectral representation of the Green's functions. The Green's function is given by

$$G(\mathbf{r}) = \frac{1}{4\pi}\frac{1}{R_{m_0,n_0}} + \widetilde{G}^{E,spatial}(\mathbf{r}) + \widetilde{G}^{E,spectral}(\mathbf{r})$$

$$-\widetilde{G}^{E,spatial}(\mathbf{0}) - \widetilde{G}^{E,spectral}(\mathbf{0}),$$

where

$$\widetilde{G}^{E,spectral}(\mathbf{r}) = \frac{1}{4A}\sum_{m=-\infty}^{\infty}\sum_{n=-\infty}^{\infty} S_{m,n}^{E,spectral},$$

$$S_{m,n}^{E,spectral} = \Bigg(e^{-k_{tmn}|z|}\operatorname{erfc}(\frac{k_{tmn}}{2E} - |z|\,E)$$
$$+ e^{k_{tmn}|z|}\operatorname{erfc}(\frac{k_{tmn}}{2E} + |z|\,E)\Bigg)\frac{\cos(\mathbf{k}_{tmn}\cdot\boldsymbol{\rho})}{k_{tmn}},$$

$$S_{0,0}^{E,spectral} = -2\left[|z|\operatorname{erf}(|z|\,E) + \frac{e^{-(|z|E)^2}}{E\sqrt{\pi}}\right],$$

$$\widetilde{G}^{E,spatial}(\mathbf{r}) = \frac{1}{4\pi}\sum_{m=-\infty}^{\infty}\sum_{n=-\infty}^{\infty} S_{m,n}^{E,spatial},$$

$$S_{m,n}^{E,spatial;} = \frac{\operatorname{erfc}(R_{m,n}E)}{R_{m,n}},$$

and

$$S_{0,0}^{E,spatial} = \frac{-\operatorname{erf}(R_{m_0,n_0}\ E)}{R_{m_0,n_0}}.$$

The gradient of the Green's function is

$$\nabla G(\mathbf{r}) = \frac{1}{4\pi}\nabla\frac{1}{R_{m_0,n_0}}$$

$$+\nabla\widetilde{G}^{E,spatial}(\mathbf{r}) + \nabla\widetilde{G}^{E,spectral}(\mathbf{r}),$$

where

$$\nabla\widetilde{G}^{E,spectral}(\mathbf{r}) = \frac{1}{4A}\sum_{m=-\infty}^{\infty}\sum_{n=-\infty}^{\infty}$$

$$[k_{tmn,x}\widehat{x} + k_{tmn,y}\widehat{y}]\, S_{m,n}^{E,spectral} + \widehat{z}T_{m,n}^{E,spectral},$$

$$S_{m,n}^{E,spectral} = -\Bigg[e^{-k_{tmn}|z|}\operatorname{erfc}(\frac{k_{tmn}}{2E} - |z|\,E)$$

$$+ e^{k_{tmn}|z|}\operatorname{erfc}(\frac{k_{tmn}}{2E} + |z|\,E)\Bigg]\frac{\sin(\mathbf{k}_{tmn}\cdot\boldsymbol{\rho})}{k_{tmn}},$$

and

$$T_{m,n}^{E,spectral} = (-e^{-k_{tmn}|z|}\operatorname{erfc}(\frac{k_{tmn}}{2E} - |z|\,E)$$

$$+ e^{k_{tmn}|z|}\operatorname{erfc}(\frac{k_{tmn}}{2E} + |z|\,E))\cos(\mathbf{k}_{tmn}\cdot\boldsymbol{\rho})\operatorname{sgn}(z)$$

$$+\frac{2E}{k_{tmn}\sqrt{\pi}}e^{-k_{tmn}|z|}e^{-\left[\frac{k_{tmn}}{2E} - |z|E\right]^2}$$

$$-\frac{2E}{k_{tmn}\sqrt{\pi}}e^{k_{tmn}|z|}e^{-\left[\frac{k_{tmn}}{2E} + |z|E\right]^2},$$

$$T_{0,0}^{E,spectral} = -\frac{\operatorname{sgn}(z)\operatorname{erf}(|z|\,E)}{2A},$$

$$\nabla\widetilde{G}^{E,spatial}(\mathbf{r}) = \frac{1}{4\pi}\sum_{m=-\infty}^{\infty}\sum_{n=-\infty}^{\infty} S_{m,n}^{E,spatial}\nabla R_{m,n},$$

$$S_{m,n}^{E,spatial} = \left[-\frac{\operatorname{erfc}(R_{m,n}E)}{R_{m,n}^2} - \frac{2Ee^{-[R_{m,n}E]^2}}{\sqrt{\pi}R_{m,n}}\right],$$

and

$$S_{0,0}^{E,spatial} = \left[\frac{\operatorname{erf}(R_{m_0,n_0}\ E)}{R_{m_0,n_0}^2} - \frac{2Ee^{-[R_{m_0,n_0}\ E]^2}}{\sqrt{\pi}\ R_{m_0,n_0}}\right].$$

If $|z - z\prime| >> \max\ (\rho_a, \rho_b)$ as occurs for evaluation of the potential far above the braid, a static spectral series approach is used to evaluate the Green's functions.

$$\widetilde{G}^{spectral}(\mathbf{r}) = \sum_{m=-\infty}^{\infty}\sum_{n=-\infty}^{\infty}\frac{\cos(\mathbf{k}_{tmn}^s\cdot\boldsymbol{\rho})S_{m,n}^{spectral}}{2A},$$

where

$$S_{m,n}^{spectral} = \frac{e^{-k_{tmn}|z|}}{k_{tmn}},$$

$$S_{0,0}^{spectral} = -|z|,$$

$$\nabla\widetilde{G}^{spectral}(\mathbf{r}) = \sum_{m=-\infty}^{\infty}\sum_{n=-\infty}^{\infty}$$

$$\left(\frac{\left[k_{tmn,x}^s\widehat{x} + k_{tmn,y}^s\widehat{y}\right]U_{m,n}^{spectral} + \widehat{z}V_{m,n}^{spectral}}{2A}\right),$$

$$U_{m,n}^{spectral} = \frac{-e^{-k_{tmn}^s|z|}}{k_{tmn}^s}\sin(\mathbf{k}_{tmn}^s\cdot\boldsymbol{\rho}),$$

$$V_{m,n}^{spectral} = -\operatorname{sgn}(z)\cos(\mathbf{k}_{tmn}^s\cdot\boldsymbol{\rho})e^{-k_{tmn}^s|z|},$$

and

$$V_{0,0}^{spectral} = -\frac{\operatorname{sgn}(z)}{2A}.$$

4 Results

We choose the point $r_0 = (0, 0, z_0)$ above the braid and use (10) and (11) to obtain the transfer capacitance for the case sources up to dipoles, quadrupoles and octopoles. The results for the total braid problem (a superposition of the uniform field and the unit voltage on the braid problem) are summarized in Table 1.

The first example considered is cable whose unit cell contains half the wires in the full Beldon unit cell as illustrated in Figure 3. As illustrated in Table 1 excellent agreement is obtained between models. The full EIGER^{TM} simulation [1] with 12 and 16 elements around the circumference gave

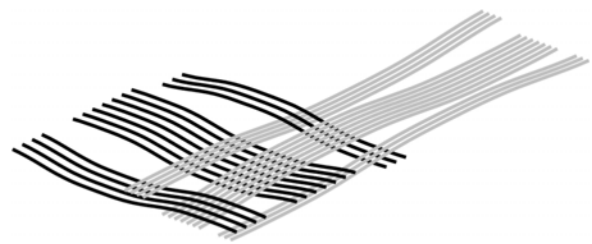

Figure 3: Cable braid model consisting of half (14+14) the wires in the unit cell of the Beldon cable. The individual lines correspond to the center lines of the wires. The wire thickness due to the radius a is not shown.

Table 1: $\phi^{tot}/(1V/m)$ for half (14+14) and full (28+28) Beldon cable with $\mathbf{r} = 8.0\widehat{\mathbf{z}}$.

	Half (14+14)	Full (28+28)
fil	$5.26\times10^{-5}m$	$-2.60\times10^{-7}m$
dip	$5.10\times10^{-5}m$	$3.60\times10^{-7}m$
quad	$4.86\times10^{-5}m$	$-7.66\times10^{-8}m$
oct	$4.87\times10^{-5}m$	$-5.72\times10^{-8}m$

$\phi^{tot}/\frac{1V}{m}$ equal to $9.11\times10^{-8}m$ and $8.67\times10^{-8}m$, respectively. The semi-emperical formula gave $1.3\times10^{-7}m$. Since coupling to a braid with high optical coverage will be dominated by magnetic flux penetration through the braid, the acuracy of the small numbers for the planar braid transfer capacitance is not a concern. A similar formulation for the magnetostatic transfer inductance will be presented in the talk but is omitted here due to space considerations.

References

[1] W. A. Johnson, L. K. Warne, L. I. Basilio, R. S. Coats, J. D. Kotulski, and R. E. Jorgenson, "Modeling of Braided Shields", Proceedings of Joint 9th International Conference on Electromagnetics in Advanced Applications ICEEA 2005 and 11th European Electromagnetic Structures Conference EESE 2005, Torino, Italy, pp. 881-884, Sept. 2005.

[2] T. F. Eibert, J. L. Volakis, D. R. Wilton, and D. R. Jackson, "Hybrid FE/BI Modeling of 3D Doubly Periodic Structures Utilizing Triangular Prismatic Elements and an MPIE Formulation Accelerated by the Ewald Transformation," IEEE Trans. Antennas and Propagat., vol. 47, no. 5, pp. 843–849, May 1999.